The ocean's gravitational potential energy budget in a coupled climate model

Article

Published Version

It is advisable to refer to the publisher's version if you intend to cite from the
work. See Guidance on citing.

www.reading.ac.uk/centaur

CentAUR

Central Archive at the University of Reading

Reading's research outputs online

The ocean's gravitational potential energy budget in a coupled climate model

E. D. Butler,[1,2] K. I. Oliver,[1] J. M. Gregory,[3] and R. Tailleux[3]

[1] This study examines, in a unified fashion, the budgets of ocean gravitational potential energy (GPE) and available gravitational potential energy (AGPE) in the control simulation of the coupled atmosphere-ocean general circulation model HadCM3. Only AGPE can be converted into kinetic energy by adiabatic processes. Diapycnal mixing supplies GPE but not AGPE, whereas the reverse is true of the combined effect of surface buoyancy forcing and convection. Mixing and buoyancy forcing thus play complementary roles in sustaining the large-scale circulation. However, the largest globally integrated source of GPE is resolved advection (+0.57 TW) and the largest sink is through parameterized eddy transports (–0.82 TW). The effect of these adiabatic processes on AGPE is identical to their effect on GPE, except for perturbations to both budgets due to numerical leakage exacerbated by nonlinearities in the equation of state. **Citation:** Butler, E. D., K. I. Oliver, J. M. Gregory, and R. Tailleux (2013), The ocean's gravitational potential energy budget in a coupled climate model, *Geophys. Res. Lett.*, *40*, 5417–5422, doi:10.1002/2013GL057996.

1. Introduction

[2] Global ocean circulation has a significant effect on the Earth's climate, but the relative importance of the processes responsible for driving global ocean circulation are still debated. It is postulated that the ocean's budget of mechanical energy, comprising kinetic energy (KE), gravitational potential energy (GPE), and the work of expansion and compression, can provide insights into the nature of this circulation and its driving processes [e.g., *Munk and Wunsch*, 1998; *Oliver and Edwards*, 2008; *Urakawa and Hasumi*, 2009; *Tailleux*, 2010; *Gregory and Tailleux*, 2011]. In this study, we focus our analysis on the ocean's GPE budget.

[3] Sources of GPE, such as turbulent diapycnal mixing [e.g., *Munk and Wunsch*, 1998] and the wind-driven upwelling of dense water [e.g., *Webb and Suginohara*, 2001], are required to sustain the meridional overturning circulation. It is a widely held idea that surface buoyancy

---

Additional supporting information may be found in the online version of this article.

[1]Ocean and Earth Science, National Oceanography Centre Southampton, University of Southampton, UK.

[2]Institute for Complex Systems Simulation, University of Southampton, UK.

[3]Department of Meteorology, University of Reading, UK.

Corresponding author: E. D. Butler, Ocean and Earth Science, National Oceanography Centre Southampton, University of Southampton Waterfront Campus, European Way, Southampton, SO14 3ZH, UK. (e.d.butler@soton.ac.uk)

forcing cannot supply this mechanical energy and that the work done by buoyancy forcing is effectively zero [*Wunsch and Ferrari*, 2004]. This is because buoyancy is gained and lost at approximately the same pressure level (i.e., the surface) and thus has a negligible effect on globally integrated GPE [*Huang and Jin*, 2006]. However, it is argued that analyzing GPE alone can produce misleading conclusions [*Hughes et al.*, 2009] and that a distinction must be made between overall GPE and the portion of this which can be converted to KE by adiabatic processes, available gravitational potential energy (AGPE). AGPE is defined to be the difference between the GPE of the physical state and the GPE of the reference state, which is a hypothetical state of minimum GPE achieved through reversible, adiabatic rearrangement of water masses [e.g., *Lorenz*, 1955; *Huang*, 2005].

[4] Not all oceanic processes affect GPE and AGPE in the same manner. Physical processes in the ocean can be identified as adiabatic or diabatic through their effects on the GPE reference state [*Winters et al.*, 1995; *Tailleux*, 2009]. Adiabatic processes are defined here (according to *Winters et al.* [1995]) as those that do not involve the transfer of heat or molecular mass between fluid parcels (and a diabatic process as one that is not adiabatic). Adiabatic processes move fluid parcels reversibly without mixing, therefore they do not alter the frequency distribution of temperature or salinity, and accordingly do not affect the GPE of the reference state. Consequently, adiabatic processes have the same effect on both GPE and AGPE. The AGPE budgets of ocean models with idealized configurations have been analyzed previously [e.g., *Toggweiler and Samuels*, 1998; *Hughes et al.*, 2009; *Saenz et al.*, 2012], and AGPE has been discussed extensively in a theoretical context by *Tailleux* [2009]. *Hughes et al.* [2009] demonstrated that spatial variations in surface buoyancy forcing can generate AGPE without generating GPE by reducing the GPE of the reference state.

[5] The ocean's major mechanical energy sources are still weakly constrained by observations [*Wunsch and Ferrari*, 2004; *Hughes et al.*, 2009] and are not well understood in realistic climate models. The KE budget of the atmosphere-ocean general circulation model (AOGCM) HadCM3 has been analyzed regionally by *Gregory and Tailleux* [2011], who found that although surface wind stress was the primary source of KE, buoyancy fluxes nevertheless represent a significant source of KE at high latitudes and in western boundary currents. In the global integral, the resolved circulation does work against the pressure gradient, indicating net conversion from KE to GPE by resolved advection. In this study, we decompose both the GPE and AGPE (hereafter (A)GPE) budgets from the control simulation of HadCM3 in a unified fashion. Based on these results, we present a framework for understanding the role of both diabatic processes, whereby turbulent diapycnal mixing

supplies GPE that is made available by buoyancy forcing, and adiabatic processes, in which large-scale advection is a primary (A)GPE source and parameterized eddies are the largest (A)GPE sink.

2. Method

[6] Model output from the control simulation of the Hadley Centre coupled AOGCM (HadCM3) is used in this study. HadCM3 is a coupled ocean-atmosphere global climate model that requires no flux adjustments to maintain a stable, reasonably realistic climate [*Gordon et al.*, 2000] and was used in both the third and fourth IPCC climate assessments. The oceanic component has a nonlinear equation of state, realistic bottom topography, a rigid lid, 20 depth levels, and a horizontal resolution of $1.25° \times 1.25°$.

[7] The local contribution to global GPE of a single model cell is defined to be equal to the volume integral of the product of density, gravity, and vertical displacement. In the fixed geometry of a volume conserving, z coordinate ocean model, cell volume V, and vertical displacement z (defined at the center of the cell) are constant. Consequently, differentiation with respect to time yields

$$\frac{\partial \text{GPE}_{(i,j,k)}}{\partial t} = g \frac{\partial \rho_{(i,j,k)}}{\partial t} V_{(i,j,k)} z_{(i,j,k)} \qquad (1)$$

in which g is the gravitational constant, ρ is the density, V is volume, z is vertical displacement, and (i, j, k) are the model cell coordinates. z must be defined relative to the surface to avoid spurious GPE generation and dissipation associated with the conservation of volume, rather than mass (see supporting information). Density is a function of potential temperature θ, salinity S, and pressure p. In a Eulerian framework, we have

$$\frac{1}{\rho_0}\frac{\partial \rho}{\partial t} = -\alpha\frac{\partial\theta}{\partial t} + \beta\frac{\partial S}{\partial t}; \quad \alpha := -\frac{1}{\rho_0}\frac{\partial\rho}{\partial\theta}, \quad \beta := \frac{1}{\rho_0}\frac{\partial\rho}{\partial S}. \quad (2)$$

[8] AGPE is defined as the difference between the GPE of the physical state and GPE of the reference state, GPE_{ref} : $\text{AGPE} = \text{GPE} - \text{GPE}_{\text{ref}}$. Reference states of minimal GPE are calculated according to the sorting algorithm devised by *Huang* [2005]. Model cells are sorted according to density and rearranged adiabatically into layers spanning the global ocean, such that the densest cell is spread across the bottom of the ocean. Variations in ocean area with depth are accounted for in this calculation. The ocean is treated as a single basin when constructing the reference state, and consequently, total AGPE may be overestimated as topographically trapped dense water masses are permitted to redistribute into the deep global ocean.

[9] Reference state GPE is defined analogously to physical state GPE with the actual vertical displacement, z, replaced by the vertical position in the reference state, z_{ref}, and in situ density, $\rho = \rho(\theta, S, p(z))$, replaced by density in the reference state, $\rho_{\text{ref}} = \rho(\theta, S, p(z_{\text{ref}}))$. The evolution of GPE_{ref} is given by

$$\frac{\partial\text{GPE}_{\text{ref}}}{\partial t} = \int g\left(\frac{\partial\rho_{\text{ref}}}{\partial t}z_{\text{ref}} + \rho_{\text{ref}}\frac{\partial z_{\text{ref}}}{\partial t}\right)\,dV. \qquad (3)$$

[10] It has been demonstrated that the second term of equation (3) integrates identically to zero [*Winters et al.*, 1995; *Tailleux*, 2009]. Therefore, we define the local contribution to global GPE_{ref} of density changes in a single model grid cell to be

$$\frac{\partial\text{GPE}_{\text{ref}(i,j,k)}}{\partial t} = g\frac{\partial\rho_{\text{ref}(i,j,k)}}{\partial t}V_{(i,j,k)}z_{\text{ref}(i,j,k)}, \qquad (4)$$

in which

$$\frac{1}{\rho_0}\frac{\partial\rho_{\text{ref}}}{\partial t} := -\alpha_{\text{ref}}\frac{\partial\theta}{\partial t} + \beta_{\text{ref}}\frac{\partial S}{\partial t};$$
$$\alpha_{\text{ref}} := -\left.\frac{1}{\rho_0}\frac{\partial\rho}{\partial\theta}\right|_{p=p(z_{\text{ref}})},$$
$$\beta_{\text{ref}} := \left.\frac{1}{\rho_0}\frac{\partial\rho}{\partial S}\right|_{p=p(z_{\text{ref}})}. \qquad (5)$$

[11] Variations in GPE_{ref} due to changes in reference state pressure are neglected in equation (5), because calculation of this term is intractable for the individual processes described below. We note that the contribution of this term to net $\partial\text{GPE}_{\text{ref}}/\partial t$ (in offline calculations not shown) is small.

[12] This study makes use of 140 years of monthly averaged model output in the calculations described above. Potential temperature and salinity tendencies due to each model process are diagnosed online. α, β, α_{ref}, β_{ref}, and z_{ref} are calculated offline using monthly averages of θ and S. We adopt the following decomposition of the temperature and salinity budgets (for which mathematical equations are given in the supporting information):

[13] 1. Buoyancy forcing (BUOY): penetrative solar radiation and fluxes of temperature and salinity due to exchange with the atmosphere and sea ice.

[14] 2. Convection (CON): convective readjustment to remove static instabilities in the water column. This term includes mixed layer deepening driven by KE released during convection and a small contribution from mixed layer mixing due to wind-driven turbulence according to the Kraus-Turner energetics parameterization [*Gordon et al.*, 2000].

[15] 3. Advection (ADV): the intercell transport of temperature and salinity due to the resolved circulation. In the global energy budget, this is often interpreted as the conversion between KE and (A)GPE. However, KE loss generally differs from both GPE gain and AGPE gain due to the nonlinear equation of state and numerical mixing in models. Locally, this term includes both divergence in the transport of GPE and local exchange between GPE and KE.

[16] 4. Diapycnal mixing (DIA): diffusive scheme representing the combined effect of turbulent advection and irreversible mixing by applying diffusivity coefficients far greater than molecular values. This is calculated according to the depth-dependent background coefficients of vertical diffusion (varying from 1.03×10^{-5} m^2 s^{-1} between surface layers to 14.68×10^{-5} m^2 s^{-1} in the abyssal ocean [*Gordon et al.*, 2000]) and monthly averaged θ, S fields.

[17] 5. Isopycnal diffusion (ISO): parameterization of along-isopycnal eddy fluxes using a constant diffusion coefficient of 1000 m^2 s^{-1} [*Gordon et al.*, 2000].

[18] 6. Gent and McWilliams (GM): parameterization of bolus fluxes due to mesoscale eddies. This represents unresolved advection in the model and is carried out by the *Visbeck et al.* [1997] implementation of the *Gent and McWilliams* [1990] parameterization. The thickness diffusion coefficient varies spatially and temporally (between an

Table 1. The Time Mean of Globally Integrated GPE, GPE_ref, and AGPE Tendencies of the HadCM3 Control Climate[a]

Term	BUOY	CON	ADV	DIA	ISO	GM	Sum
GPE	+0.26 ± 0.00	−0.39 ± 0.01	+0.57 ± 0.02	+0.33 ± 0.00	−0.07 ± 0.00	−0.82 ± 0.01	−0.13 ± 0.02
GPE_ref	−0.46 ± 0.02	+0.04 ± 0.01	−0.02 ± 0.02	+0.44 ± 0.01	−0.11 ± 0.02	−0.08 ± 0.01	−0.18 ± 0.02
AGPE	+0.72 ± 0.02	−0.44 ± 0.01	+0.59 ± 0.02	−0.12 ± 0.01	+0.04 ± 0.02	−0.74 ± 0.01	+0.05 ± 0.02

[a]Calculated using monthly averaged data and then averaged over the 140 year sample period (in units of TW = 10^{12} W). Positive values indicate energy sources, whereas negative values indicate energy sinks; values preceded by ± indicate the standard deviation of the decadal mean tendencies.

imposed minimum of 350 m^2 s^{-1} and a maximum of 2000 m^2 s^{-1}) so as to enhance mixing in regions of baroclinic instability [*Gordon et al.*, 2000].

3. Results

3.1. The Global Energy Balance

[19] The globally integrated GPE, reference state GPE, and AGPE budgets are presented in Table 1. There is a large drift (that is, a nonzero budget sum) in GPE, but not AGPE, which we return to in section 4. Within our global decomposition, advection is a primary source of GPE (+0.57 TW) and of AGPE (+0.59 TW). Physically, this implies a net conversion of KE into (A)GPE, similarly as was found by *Toggweiler and Samuels* [1998] and *Gnanadesikan et al.* [2005]. This indicates that globally, work done by Ekman transport and wind-driven upwelling against the horizontal pressure gradient (raising dense fluid parcels and pushing down light fluid parcels) dominates over buoyancy-driven flows driven by horizontal pressure gradients, as discussed by *Gregory and Tailleux* [2011].

[20] The largest sink of GPE (−0.82 TW) and AGPE (−0.74 TW) is through the parameterized bolus fluxes due to eddies. These act to flatten isopycnals (surfaces of equal density). This implies a downwelling of dense water and an upwelling of light water and acts as a sink of (A)GPE. Our result is larger in magnitude than the work of the bolus velocity estimated by *Aiki and Richards* [2008] from an eddy-resolving ocean model (−0.46 TW). However, the ratio of GPE generation by the resolved circulation (cf. the mean isopycnal velocity in *Aiki and Richards* [2008]) to GPE dissipation by the bolus velocity is consistent between studies. This is suggestive of an enhanced energy cycle in HadCM3.

[21] Diapycnal mixing is a leading order GPE source (+0.33 TW). By mixing warmer surface waters down and colder deep waters up, the GPE of the ocean is increased. This is a diabatic process and has a comparable, but not identical, effect on the GPE of the reference state as it does on the GPE of the actual state. Since the reference state is stably stratified, mixing raises its center of mass and increases GPE_ref (+0.44 TW). Conversely, diapycnal mixing is a (small) sink of AGPE (−0.12 TW).

[22] It has been shown previously that surface buoyancy fluxes can play an active energetic role in sustaining global ocean circulation by generating AGPE [*Tailleux*, 2009]. This notion is supported by our analysis, in which surface buoyancy forcing is the largest source of AGPE (+0.72 TW). Previous studies [e.g., *Huang and Jin*, 2006] have indicated that surface buoyancy forcing is not a significant source of GPE, even taking nonlinearities in the equation of state into account. However, in HadCM3, surface buoyancy fluxes are

a GPE source of +0.26 TW, comparable in magnitude to the effects of diapycnal diffusion. This is principally due to solar radiation penetrating to subsurface model layers, an effect neglected in *Hughes et al.* [2009].

[23] In contrast, convective readjustment is a GPE (−0.39 TW) and AGPE (−0.44 TW) sink; downwelling density and lowering the center of mass of the ocean. Convection is usually a response to buoyancy forcing, and the combined effect of the two processes is to produce AGPE (+0.28 TW) but consume GPE (−0.13 TW).

[24] Finally, isopycnal diffusion is a small sink of GPE and source of AGPE. If the equation of state were linear, isopycnal diffusion would not change GPE since it is only mixing water masses of equal density. With a nonlinear equation of state, cabbeling and thermobaricity can destroy or create buoyancy, leading to these small globally integrated effects.

3.2. Local Contributions to the Global Energy Balance

[25] Figure 1 presents the zonally and vertically integrated (A)GPE tendencies as a function of latitude. The budgets are in approximate local balance. If the density of a water column is increased, the GPE of the water column is decreased (and vice versa). The deeper a density change takes place, the greater the energetic effect. In addition to local generation and dissipation, GPE can also be fluxed between water columns. AGPE is more complicated to interpret by latitude. Processes that increase the density of water lying above its reference level in the physical ocean increase AGPE, while processes that decrease the density of such water decrease AGPE. The reverse is true for water below its reference level. The AGPE budget is dominated by regions of large $|z - z_{ref}|$ with the most significant local contributions in the Southern Ocean, the high-latitude North Atlantic, the Arctic, and the Mediterranean Sea; areas in which dense water is significantly higher in the physical ocean than in the reference state (as depicted in the supporting information, Figure S1). These findings are consistent with the AGPE distribution mapped by *Huang* [2005]. Large areas of low-latitude ocean are almost negligible in terms of AGPE generation and dissipation, despite being evident in the GPE budget. This is reflected in Figure 1b.

[26] The dominant role of the Southern Ocean in the global energy budget is immediately apparent (as observed in the HadCM3 KE budget [*Gregory and Tailleux*, 2011] and the GPE budget of an idealized ocean model [*Urakawa and Hasumi*, 2009]). The primary balance is between the generation of (A)GPE through advection and the removal of (A)GPE through parameterized eddy fluxes. Across most of this region, wind-driven upwelling deflects isopycnals and raises dense water toward the surface, creating GPE. Mesoscale eddies oppose this, acting to flatten isopycnals.
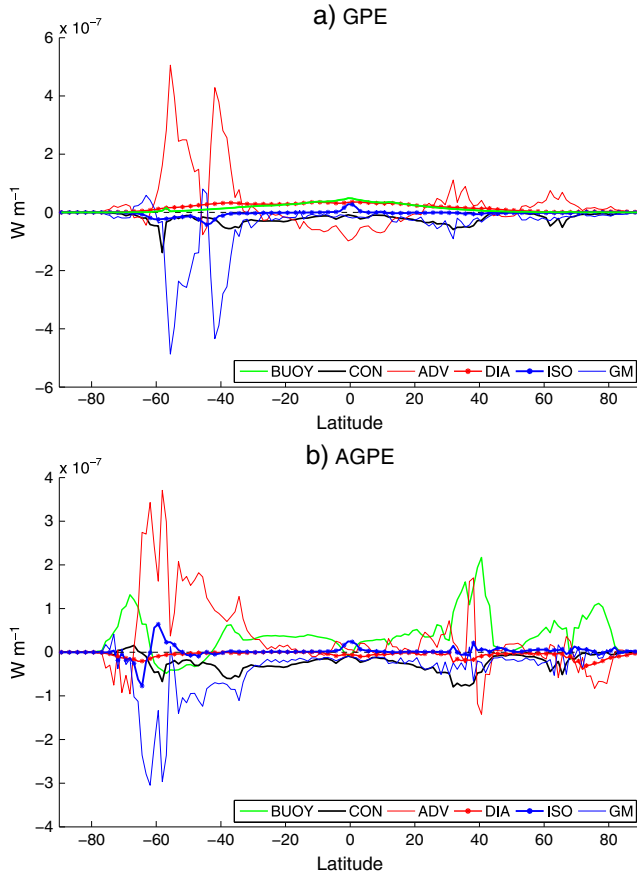
Figure 1. The zonally and vertically integrated (a) GPE and (b) AGPE tendencies due to surface buoyancy forcing (BUOY), convection (CON), advection (ADV), diapycnal diffusion (DIA), isopycnal mixing (ISO), and Gent and McWilliams mixing (GM) in the HadCM3 control climate, plotted as a function of latitude. Note that each graph has a different scale on the vertical axis. Positive values indicate local increases in energy, and negative values indicate local decreases.

[27] Neglecting numerical leakage and the variable compressibility of seawater, the GPE tendency due to advection is well approximated by

$$\left.\frac{\partial \text{GPE}}{\partial t}\right|_{\text{ADV}} \approx \int -\nabla \cdot (\rho g\, z\mathbf{u}) + \rho g w \, dV \qquad (6)$$

in which ρ is the density, g is the gravitational constant, $\mathbf{u}$ is velocity, and w is vertical velocity. Therefore, this term includes both divergence of GPE transport and local generation and dissipation. The divergence term vanishes in the global integral but not when integrated regionally. Consequently, the local change in GPE due to the resolved circulation can appear counterintuitive. For example, advection decreases GPE at low latitudes and increases GPE at high northern latitudes, whereas one might expect to see a positive peak in GPE generation through advection at low latitudes as equatorial upwelling draws denser water to the surface. This discrepancy is due to divergence in the GPE transport as GPE generated at low latitudes, in part by diabatic processes, is advected to high northern latitudes.

[28] Similarly, GPE that is generated through wind-driven upwelling at the southern boundary of the Antarctic Circumpolar Current (ACC) is transported northward, with the resulting divergence producing a small local decrease in GPE due to advection. Conversely, convergence of GPE at the northern boundary of the ACC contributes to the local increase in GPE due to advection. The net effect of advection across the ACC is to generate (A)GPE. The ACC is approximately centered at 45°S west of Kerguelen and 55°S east of Kerguelen producing the two peaks visible in Figure 1a.

[29] GPE gain through diapycnal diffusion is greatest in low-latitude equatorial regions where vertical stratification is strongest (implying larger diffusive fluxes). In this region, buoyancy forcing is a significant source of GPE due to the intensity of penetrative solar radiation. Isopycnals in the low-latitude ocean are relatively horizontal, and the Gent and McWilliams parameterization plays little role.

[30] At mid to high latitudes, convection is a sink of (A)GPE due to readjustments occurring in the mixed layer (triggered by surface cooling), with contributions at 60°N and 60°S due to the effects of convection extending deeper into the ocean. At high latitudes, buoyancy forcing is a substantial source of AGPE in both hemispheres through the surface cooling of already dense water.

[31] The spike in activity in the AGPE budget at 40°N is due to the significant displacement of the Mediterranean Sea in the reference state. The connection between the Mediterranean and the global ocean is restricted by a shallow sill. It has been suggested that the adiabatic redistribution of topographically restricted waters to the deep ocean is unrealistic and that the reference state calculated may not be physically attainable by the ocean [*Huang*, 2005]. However, we find that the dominant controls on the AGPE budget in this region (advection and surface buoyancy forcing) are predominantly acting on waters lying above sill depth. These waters can adiabatically redistribute to the deep ocean without any energetic expense, and it is thus hard to justify their exclusion from the global (A)GPE budget. It should be noted that exchanges between the Mediterranean Sea and the Atlantic Ocean are parameterized in HadCM3 [*Gordon et al.*, 2000].

4. Discussion

[32] We have shown that in the control simulation of the coupled climate model HadCM3, the ocean's (A)GPE budgets are dominated by advection in the ACC but that diabatic processes play a major role elsewhere. Buoyancy forcing, principally at high latitudes, is a source of AGPE at the expense of background GPE, whereas diapycnal mixing results in a gain of background GPE, principally at low latitudes. Since the combined effect of these processes is a net gain in (A)GPE, advection must be a net sink at steady state. However, *Gregory and Tailleux* [2011] found that advection was a net sink of kinetic energy and by inference a net source of (A)GPE in HadCM3. These results can be reconciled by distinguishing between resolved and unresolved advection (the parameterization of eddy mass fluxes) in climate models. The AGPE released by unresolved advection is implicitly assumed to be lost to the system [*Marshall and Naveira Garabato*, 2008] such that only resolved advection appears in the kinetic energy budget. However, unresolved advection is the largest term in both the GPE and AGPE budgets, providing the sink that balances the sources due to diabatic processes and resolved advection. The effect of
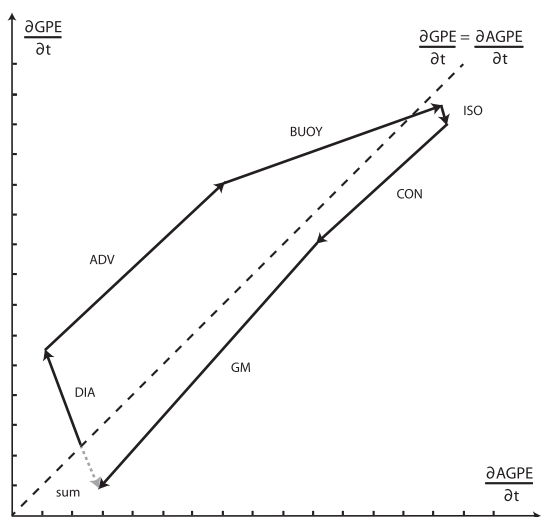
Figure 2. (A)GPE tendencies (as quoted in Table 1) depicted together on a plot of $\partial GPE/\partial t$ against $\partial AGPE/\partial t$. Positive vector components imply an increase in energy. The dashed line indicates $\partial GPE/\partial t = \partial AGPE/\partial t$. Ticks are at 0.1 TW intervals.

eddies is strongest across the steep isopycnal slopes of the ACC, and the global budgets are dominated by the residual balance between resolved wind-driven upwelling and unresolved advection in that region.

[33] Figure 2 illustrates the qualitatively different roles of adiabatic and diabatic processes using a plot of $\partial GPE/\partial t$ against $\partial AGPE/\partial t$. Vectors representing adiabatic processes must, by definition, act parallel to the line $\partial GPE/\partial t = \partial AGPE/\partial t$, since they do not change the reference state, whereas diabatic processes may have a component perpendicular to the line. Advection is an adiabatic process in the physical ocean, and it is often treated as such in the analysis of output from numerical models [e.g., *Hughes et al.*, 2009]. In practice, numerical schemes for representing advection lead to spurious mixing of water masses [*Griffies et al.*, 2000]. Figure 2 shows that both resolved and unresolved advections have small diabatic components in HadCM3, which could be caused either by cabbeling resulting from numerical isopycnal mixing or numerical diapycnal mixing. The negative sign of $\partial GPE_{ref}/\partial t$ is consistent with the former hypothesis as diapycnal mixing should be a source of reference state GPE (by virtue of its stable stratification). Conversely, cabbeling, resulting from spurious isopycnal mixing, leads to water mass densification and a sink of GPE.

[34] Though convection is carried out through an intrinsically diabatic parameterization (mixing fluid layers down through the water column until stable stratification is achieved), it has the appearance of an adiabatic process in our (A)GPE energetics framework. This is because the convective scheme mixes fluid parcels of very similar density and consequently, at very similar depths in the reference state. In effect, convective columns in the physical ocean are vertically condensed in the reference state and thus have little impact on global GPE_ref.

[35] Finally, there is a significant drift in GPE in the HadCM3 control simulation, but only a small drift in AGPE. The ongoing change in GPE (due to a 0.03°C century⁻¹ decrease in global mean temperature and a 0.001 psu

century⁻¹ increase in global mean salinity) might be considered surprising because both the ocean and climate states in HadCM3 have stabilized (as evidenced by the 0.01 Sv century⁻¹ trend in maximum Atlantic overturning stream function; standard deviation 1.06 Sv). However, since this GPE loss is not associated with a loss of AGPE, it does not leave a dynamic signature.

[36] Our results underline the importance of mesoscale processes for ocean energetics, with the caveat that the representation of eddy fluxes in HadCM3 is highly simplified. This highlights the need to understand their effect in global eddy-permitting climate models, but such simulations will present the challenge of distinguishing between large-scale and mesoscale advection in the (A)GPE budgets. Our expectation is that most (A)GPE loss (associated with unresolved advection in HadCM3) will be captured by resolved advection in an eddy-permitting model, such that resolved advection would become an (A)GPE sink balancing the effects of diapycnal mixing and buoyancy forcing. Indeed, a recent study by *Saenz et al.* [2012] using an idealized eddy-permitting ocean model with a linear equation of state supports this assertion, finding that in almost all their experimental configurations, net energy conversion is from AGPE to KE. Failure to distinguish between the two scales could hide large adiabatic contributions to the ocean's energy budget.

References

Aiki, H., and K. J. Richards (2008), Energetics of the Global Ocean: The role of layer-thickness form drag, *J. Phys. Oceanogr.*, *38*(9), 1845–1869, doi:10.1175/2008JPO3820.1.

Gent, P., and J. McWilliams (1990), Isopycnal mixing in ocean circulation models, *J. Phys. Oceanogr.*, *20*, 150–155.

Gnanadesikan, A., R. D. Slater, P. S. Swathi, and G. K. Vallis (2005), The energetics of ocean heat transport, *J. Clim.*, *18*(14), 2604–2616, doi:10.1175/JCLI3436.1.

Gordon, C., C. Cooper, C. A. Senior, H. Banks, J. M. Gregory, T. C. Johns, J. F. B. Mitchell, and R. A. Wood (2000), The simulation of SST, sea ice extents and ocean heat transports in a version of the Hadley Centre coupled model without flux adjustments, *Clim. Dyn.*, *16*(2-3), 147–168.

Gregory, J. M., and R. Tailleux (2011), Kinetic energy analysis of the response of the Atlantic meridional overturning circulation to CO2-forced climate change, *Clim. Dyn.*, *37*(5-6), 893–914, doi:10.1007/s00382-010-0847-6.

Griffies, S., R. Pacanowski, and R. Hallberg (2000), Spurious diapycnal mixing associated with advection in a z-coordinate ocean model, *Mon. Wea. Rev.*, *128*, 538–564.

Huang, R. X. (2005), Available potential energy in the world's oceans, *J. Mar. Res.*, *63*(1), 141–158, doi:10.1357/0022240053693770.

Huang, R. X., and X. Jin (2006), Gravitational potential energy balance for the thermal circulation in a model ocean, *J. Phys. Oceanogr.*, *36*(7), 1420–1429, doi:10.1175/JPO2914.1.

Hughes, G. O., A. M. C. Hogg, and R. W. Griffiths (2009), Available potential energy and irreversible mixing in the meridional overturning circulation, *J. Phys. Oceanogr.*, *39*(12), 3130–3146, doi:10.1175/2009JPO4162.1.

Lorenz, E. N. (1955), Available potential energy and the maintenance of the general circulation, *Tellus*, *7*(2), 157–167, doi:10.1111/j.2153-3490.1955.tb01148.x.

Marshall, D. P., and A. C. Naveira Garabato (2008), A conjecture on the role of bottom-enhanced diapycnal mixing in the parameterization of geostrophic eddies, *J. Phys. Oceanogr.*, *38*(7), 1607–1613, doi:10.1175/2007JPO3619.1.

Munk, W., and C. Wunsch (1998), Abyssal recipes II : Energetics of tidal and wind mixing, *Deep Sea Res.*, *45*, 1977–2010.

Oliver, K. I. C., and N. R. Edwards (2008), Location of potential energy sources and the export of dense water from the Atlantic Ocean, *Geophys. Res. Lett.*, *35*, L22604, doi:10.1029/2008GL035537.

Saenz, J. A., A. M. Hogg, G. O. Hughes, and R. W. Griffiths (2012), The mechanical power input from buoyancy and wind in an ocean model, *Geophys. Res. Lett.*, *39*, L13605, doi:10.1029/2012GL052035.

Tailleux, R. (2009), On the energetics of stratified turbulent mixing, irreversible thermodynamics, Boussinesq models, and the ocean heat engine controversy, *J. Fluid Mech.*, *638*, 339–382.

Tailleux, R. (2010), Entropy versus APE production: On the buoyancy power input in the oceans energy cycle, *Geophys. Res. Lett.*, *37*, L22603, doi:10.1029/2010GL044962.

Toggweiler, J., and B. Samuels (1998), On the ocean's large-scale circulation near the limit of no vertical mixing, *J. Phys. Oceanogr.*, *28*, 1832–1852.

Urakawa, L. S., and H. Hasumi (2009), The energetics of global thermohaline circulation and its wind enhancement, *J. Phys. Oceanogr.*, *39*(7), 1715–1728, doi:10.1175/2009JPO4073.1.

Visbeck, M., J. Marshall, T. Haine, and M. Spall (1997), Specification of eddy transfer coefficients in coarse-resolution ocean circulation models*, *J. Phys. Oceanogr.*, *27*, 381–402.

Webb, D., and N. Suginohara (2001), Oceanography: Vertical mixing in the ocean, *Nature*, *409*(6816), 37.

Winters, K., P. Lombard, and J. Riley (1995), Available potential energy and mixing in density-stratified fluids, *J. Fluid Mech.*, *289*, 115–128.

Wunsch, C., and R. Ferrari (2004), Vertical mixing, energy, and the general circulation of the oceans, *Annu. Rev. Fluid Mech.*, *36*(1), 281–314, doi:10.1146/annurev.fluid.36.050802.122121.